Supporting Information

pH-Dependent Morphology and Optical Properties of Lysine-Derived Molecular Biodynamer

Sangeun Lee,[a,b] Cansu Kaya,[a,c] Hongje Jang,[d] Marcus Koch,[e] Brigitta Loretz,[b] Eric Buhler,[f] Claus-Michael Lehr,[b,c] and Anna Katharina Herta Hirsch[a,c]**

[a.] Department for Drug Design and Optimization, Helmholtz Institute of Pharmaceutical Research Saarland (HIPS) – Helmholtz Centre for Infection Research (HZI), Campus E 8.1, 66123 Saarbrücken, Germany

[b.] Department for Drug Delivery, HIPS – HZI, Campus E8.1, 66123 Saarbrücken, Germany

[c.] Department of Pharmacy, Saarland University, 66123, Saarbrücken, Germany

[d.] Third Institute of Physics, Georg-August-Universität, Friedrich-Hund-Platz 1, 37077 Göttingen, Germany

[e.] INM-Leibniz-Institute for New Materials, Campus D2.2, Saarland University, 66123 Saarbrücken, Germany

[f.] Laboratoire Matière et Systèmes Complexes (MSC), UMR 7057, University of Paris (Paris Diderot), Bâtiment Condorcet, 75205 Paris Cedex 13, France

Corresponding Authors*

E-mail: Claus-Michael.Lehr@helmholtz-hips.de

Anna.Hirsch@helmholtz-hips.de

Experimental methods

Experimental Method

1. General methods and instrumentation

All reagents were used from commercial suppliers without further purification. Procedures were not optimized regarding yield. NMR spectra were recorded on a Bruker AV 500 (500 MHz) spectrometer. Liquid chromatography-Mass spectrometry was performed on a SpectraSystems-MSQ LCMS system (Thermo Fisher, Dreieich, Germany). Flash chromatography was performed using the automated flash chromatography system CombiFlash Rf+ (Teledyne Isco, Lincoln, NE, USA) equipped with RediSepRf silica columns (Axel Semrau, Sprockhövel Germany) or Chromabond Flash C18 columns (Macherey-Nagel, Düren, Germany). Purity of compounds synthesized by us was determined by LC-MS using the area percentage method on the UV trace recorded at a wavelength of 254 nm and found to be >95%.

2. Synthesis

All the monomers and biodynamer was synthesized according to a literature procedure.[1-3]

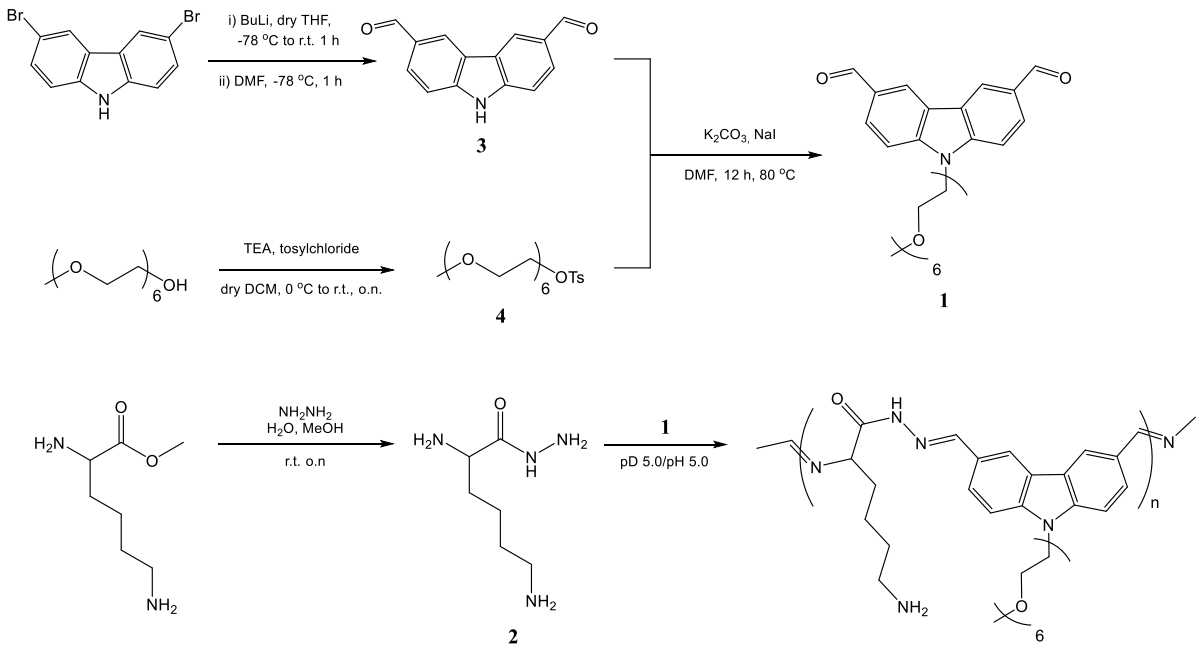

Figure S1. Overall synthesis scheme of the biodynamer

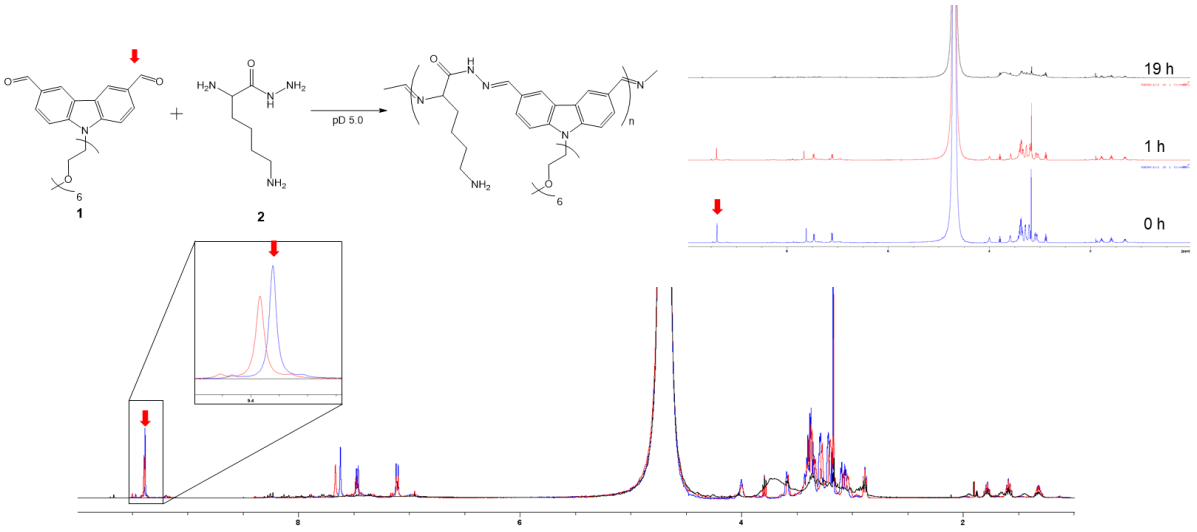

Figure S2. ^{1}H-NMR of biodynamer (500 MHz, 100 mM *d*-acetate buffer). Aldehyde proton peak (marked) was monitored by reaction time (0 h, 1 h, and 19 h).

3. Evaluation of the physicochemical property changes by polymerization

3.1. Size measurement of the micelles and the biodynamers

Sizes of the carbazole monomer micelles and the biodynamers were measured using dynamic light scattering (DLS). For preparing the carbazole monomer micelles, the monomer was dissolved in methanol or acetonitrile (200 mM). The resulting solution was added dropwise to the 100 mM acetate buffer (pH 5.0). The ratio between the organic phase (methanol or acetonitrile) and buffer was set to 1:10. After stirring the mixture for 24 hours at r.t. and removing the organic solvent, the size of the monomer particle was (10 mM in acetate buffer) measured using DLS. Each of the particles was measured using Zetasizer Nano ZSP (Malvern), observed from 173° backlight scattering.

3.2. Morphology observation using transmission electron microscopy (TEM)

TEM images of the carbazole monomer micelles were obtained using a JEM-2011 (JEOL, Akishima, Japan). 20 mM of the carbazole monomer micelles was deposited on a carbon film on 400 mesh copper grids (S160-4, Plano, Germany). After drying for 24 hours in a desiccator, the grid on the TEM holder was inserted into the TEM. The measurement was performed at a voltage of 120 kV.

Cryo-TEM images of the biodynamer were obtained using a JEM-2100 LaB6 (JEOL, Akishima, Japan). A droplet (3 µL) of the molecular biodynamer solution (10 mg/ml, in 10 mM acetate buffer (pH 5.0)) was placed on a S147-4 holey carbon film (Plano, Germany) and blotted to a thin liquid film for 2 s. Afterward the sample was plunged at T= 108 K into liquid ethane using a Gatan (Pleasonton, USA) CP3 cryo plunge system and transfered under liquid nitrogen to a

Gatan 914 cryo-TEM holder operating at T= 100 K. Then cryo-TEM measurement were performed at an accelerating voltage of 200 kV at low-dose conditions.

3.3. Morphology analysis by small angle neutron scattering (SANS)

SANS experiments were performed on the D11 beamline at Institut Laue-Langevin at Grenoble (ILL, France). An incident wavelength, λ, of 6 Å was used for 3 sample-to-detector distances (1.4, 8, and 36 m), allowing to access a total range for the magnitude of the scattering vector q varying between 0.00146 $Å^{-1}$ and 0.4074 $Å^{-1}$.[4] The scattering vector is defined by $q = 4\pi/\lambda \sin(\theta/2)$, where θ is the scattering angle. Data were corrected for empty cell scattering, electronic background and detector response and then converted to absolute scale (cm^{-1}) using normalization by the attenuated direct beam classical method.

For a polymer solution we usually write the scattered intensity $I(q)$ (cm^{-1}) as:[5]

$$I(q) = \frac{1}{V}\frac{d\sigma}{d\Omega} = k^2 c N_a g(q,c) = k^2 c N_a [g_1(q) + c g_2(q)] \quad (1)$$

V (cm^{-3}) is the sample volume and, $\frac{d\sigma}{d\Omega}$ (cm^2), the scattering cross-section. $g_1(q)=NP(q)$ is a dimensionless intramolecular term, where $P(q)$ is the chain form factor such as $P(0)=1$ and N, its degree of polymerization. $cg_2(q)$ is a dimensionless intermolecular term. k^2 (cm^2) represents the contrast factor; c (in $mol.cm^{-3}$), the monomer concentration; N_a (mol^{-1}), the Avogadro's number. The scattered intensity could also be written as:

$$I(q) = k^2 c N_a g_1(q) \left[1 + c\frac{g_2(q)}{g_1(q)}\right] = k^2 c N_a g_1(q) S(q) \quad (2)$$

allowing to define a dimensionless effective structure factor: $S(q) = 1 + c\frac{g_2(q)}{g_1(q)}$.

By introducing, $\Delta\rho^2 = (\rho_{monomer} - \rho_{solvent})^2$ (cm^{-4}), the difference in scattering length density between polymer and solvent, instead of the contrast factor k^2, V_P (cm^3) the dry volume of the polymer, instead of the degree of polymerization N, and the monomer volume fraction ϕ instead of the monomer concentration c, we can still write:

$$I(q) = \frac{1}{V}\frac{d\sigma}{d\Omega} = \Delta\rho^2\ \phi\ V_P\ P(q)\ S(q) \quad (3)$$

The scattering length densities of the monomer, $\rho_{monomer}$, and that of the solvent molecule, $\rho_{solvent}$, are determined from their known chemical compositions, using the relation:

$$\rho = \sum n_i b_i / N_a m v \quad (4)$$

where N_a is the Avogadro's number; b_i, the scattering length of the n_i atoms of the monomer or the solvent molecule; m and v, the molar mass and specific volume of the monomer or the solvent molecule, respectively. The specific volume of the monomers has been determined previously and taken to be equal to 1/1.46=0.685 cm^3/g.[1,3] That of the solvent (deuterated water) is 1/1.11=0.9 $cm^3\ g^{-1}$. We obtained $\Delta\rho^2 = 2.07 \times 10^{21}$ cm^{-4} for the dynamers.

In the qR_g<1 regime, a classical Guinier analysis was used to determine the radius of gyration, R_g, of the polymers:

$$1/I(q) = 1/I(0)\left(1 + \frac{q^2 R_g^2}{3}\right) \quad (5)$$

3.4. Morphology analysis by light scattering (LS)

The measurements used a 3D dynamic light scattering (DLS) spectrometer (LS Instruments, Fribourg, Switzerland) equipped with a 25 mW HeNe laser (JDS uniphase) operating at λ=632.8 nm, a two channel multiple tau correlator (1088 channels in autocorrelation), a variable-angle detection system, and a temperature-controlled index matching vat (LS Instruments). The scattering spectrum was measured using two single mode fibre detections and two high sensitivity APD detectors (Perkin Elmer, model SPCM-AQR-13-FC).

Fluctuations in the scattered intensity with time $I(q,t)$ (also called count rate), measured at a given scattering angle θ or equivalently at a given scattering wave vector $q = (4\pi n/\lambda)\sin(\theta/2)$, are directly reflecting the so-called Brownian motion of the scattering particles. In dynamic light scattering (DLS), the fluctuation pattern is translated into the normalized time autocorrelation function of the scattered intensity, $g^{(2)}(q,t)$ defined as:

$$g^{(2)}(q,t) = \frac{\langle I(q,0)I(q,t)\rangle}{\langle I(q,0)\rangle^2} \quad (6)$$

It is related to the so-called dynamic structure factor (or concentration fluctuations autocorrelation function), $g^{(1)}(q,t)$, via the Siegert relation:

$$g^{(2)}(q,t) - 1 = \beta\left|g^{(1)}(q,t)\right|^2 \quad (7)$$

Where β is the coherence factor, which in our experiments is varying between 0.80 and 0.95, depending on the samples and the setup geometry. The normalized dynamical correlation function, $g^{(1)}(q,t)$, of concentration fluctuations is defined as:

$$g^{(1)}(q,t) = \frac{\langle \delta c(q,0)\delta c(q,t)\rangle}{\langle \delta c(q,0)^2\rangle} \quad (8)$$

Where $\delta c(q,t)$ and $\delta c(q,0)$ represent fluctuations of the concentration at time t and zero, respectively. Examples of correlation functions are given in Figure S3. The distribution of decay rates $G(\Gamma)$ was determined using the CONTIN algorithm based on the inverse Laplace transform of $g^{(1)}(q,t)$:

$$g^{(1)}(q,t) = \int_0^\infty G(\Gamma)\exp(-\Gamma t)\, d\Gamma \quad (9)$$

For a diffusive process, with characteristic time, τ = 1/Γ, inversely proportioned to q^2, $g^{(1)}(q,t) \sim \exp(-Dq^2t)$, with D the mutual diffusion coefficient. The Stokes-Einstein relation allows one to determine the hydrodynamic radius R_h of the scattered objects; $R_h = kT/6\pi\eta D$, if the temperature T and solvent viscosity η are known (here η = 1.002 cP at 20 °C for water). In our

experiments, solutions were characterized by a single relaxation mechanism. We have then also adopted the cumulant analysis:

$$lng^{(1)}(q,t) = k_0 - k_1 t + \frac{k_2}{2} t^2 + \cdots (10)$$

Where $k_1 = 1/\langle\tau\rangle$ and k_2/k_1^2 represents the polydispersity index. The extrapolation of $(\langle\tau\rangle q^2)^{-1}$ to $q = 0$ yields the mutual diffusion coefficient D.

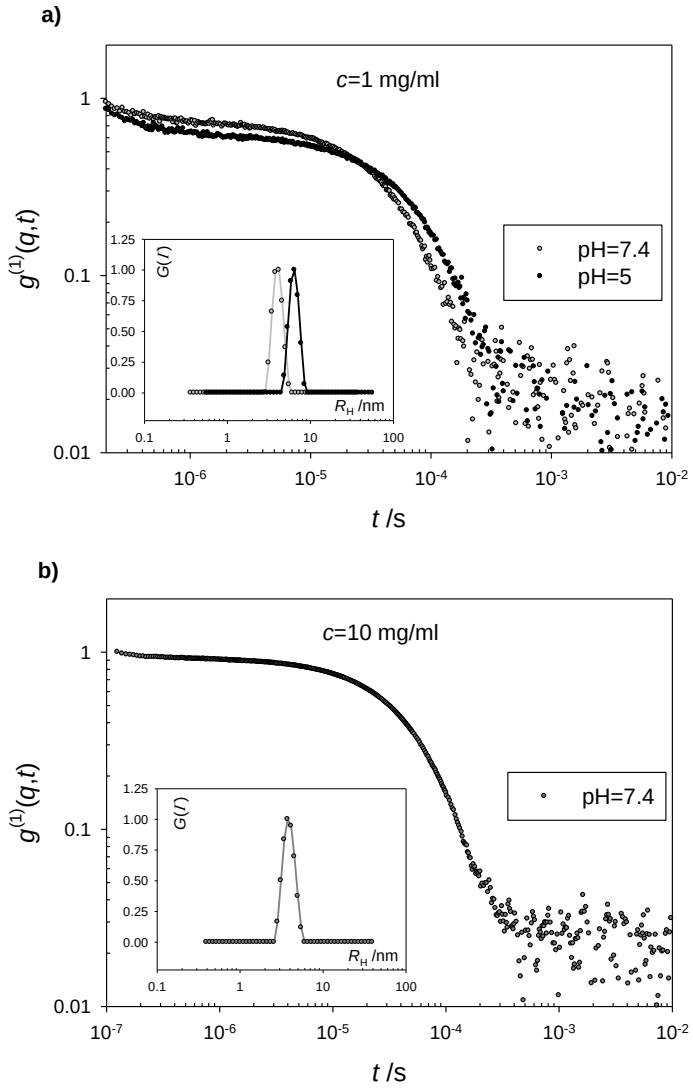

Figure S3. Concentration fluctuations autocorrelation functions obtained from dynamic light scattering (DLS) experiments at scattering angle of 90° for polymers at a) 1 mg/mL (pH 5.0 and 7.4) and b) 10 mg/mL (pH 7.4). The insets represent the size distribution obtained by applying the Contin method to the data.

In static light scattering (SLS) experiments, the excess of scattered intensity is measured with respect to the solvent. The so-called excess Rayleigh ratio was deduced using a toluene sample

reference for which the excess Rayleigh ratio is well-known ($R_{toluene}$ = 1.3522×10^{-5} cm^{-1} at 633 nm):

$$R_{solute}(cm^{-1}) = \frac{I_{solution}-I_{solvent}}{I_{toluene}} \times \left(\frac{n}{n_{toluene}}\right)^2 \times R_{toluene} \quad (11)$$

The usual equation for absolute light scattering combines the form factor *P(q)*, the structure factor *S(q)* and the weight-averaged molecular weight M_w of the scattered objects:

$$R(q) = \frac{4\pi^2 n^2}{N_a \lambda^4}\left(\frac{dn}{dC}\right)^2 C M_W P(q) S(q) \quad (12)$$

where $K = 4\pi^2 n^2 (dn/dC)^2 / N_A \lambda^4$=2.47514×10^{-7} cm^2.g^{-2}.mol is the scattering constant (refractive index n = 1.33 for water solvent at 20 °C) and N_a the Avogadro's number. A refractive index increment of dn/dC = 0.185 cm^3/g determined previously for similar molecules was considered to be a sufficient approximation.[6-8] Extrapolation of the Rayleigh ratio to zero-q, with $P(q=0)$=1 and $S(q)$~1 in dilute regime, allows determination of M_w (see Figure S4):

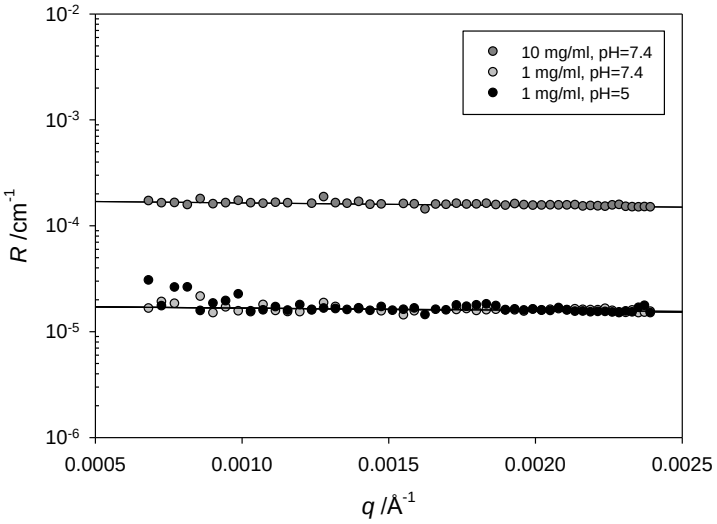

Figure S4. Static light scattering (SLS) experiments: variation of *R* with *q* in the Guinier plateau (qR_g<1) allowing determination of the apparent weight-averaged molecular weight M_w of the polymers (see equation 12).

3.5. Absorption and emission shifts by the polymerization

Absorption and emission changes were measured by the polymerization using Infinite M200 Pro (Tecan, Zürich, Switzerland). The mixture of the monomers was prepared in 100 mM acetate buffer (pH 5.0) with a final concentration of 10 mM. At each time point (0, 2, 4, 10, 18, and 24 hours), the plate reader monitored emissions of the solution (200 μL) in 96 well plates scanning from 380 nm to 700 nm with an excitation of 350 nm. It scanned with an emission wavelength step of 5 nm, and 25 flashes. To measure the absorption, above solutions were scanned from 320 to 500 nm.

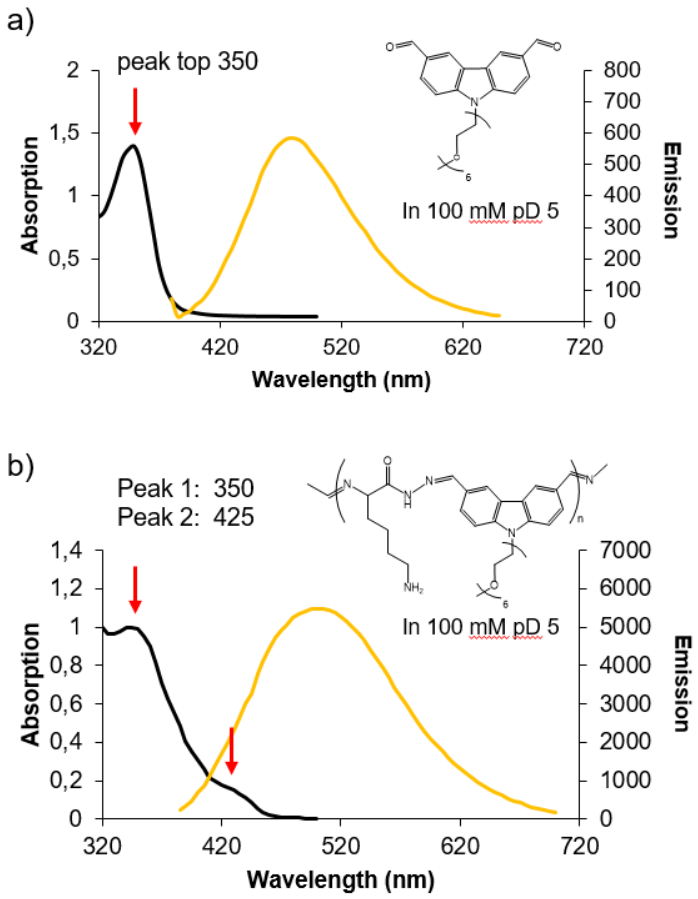

Figure S5. Absorption and emission spectra of hexaethylene glycol conjugated carbazole dicarboxaldehyde (a), and the biodynamer (b).

4. pH effect on the molecular biodynamer

4.1. pH-dependent emission shift

4.1.1. Emission shift of biodynamer upon pH change

Emission and absorption of the biodynamer at different pH were measured using Infinite M200 Pro (Tecan, Zürich, Switzerland). First, we prepared solutions with various pH (3, 5, 6, 7.4, 9, 11, and 13). We have adjusted pH of 10 mM acetate buffer (pH 5.0) using 10 M NaOH and 1 M HCl for preparing the acidic pH solutions (pH 3 and pH 6). For preparing basic pH solutions (pH 9, 11 and 13), 10 M NaOH added into 10 mM phosphate buffer (pH 7.4). The biodynamer, prepared in 10 mM acetate buffer (pH 5.0), was diluted to 1 mg/mL using the prepared solutions with various pH. The plate reader scanned emission of the biodynamer solutions (200 µl in a 96 well plate) from 380 nm to 700 nm, with an excitation at 350 nm. The maximum intensity of each obtained spectrum normalized their spectrum.

4.1.2. Ratio calculation between protonated and unprotonated carbazoles in the biodynamer

We proceeded signal fitting by two steps i)model curve fitting of each single species and ii)ratio calculation for mixtures of dual-species. All the calculations processed using the homebuilt program based on MatLab R2019.

In the first step, the two model spectra were fitted using the signals obtained at pH 3 and 13. Each model spectrum was composed of two Gaussian functions to describe the shape of the original spectra precisely (equation 13). In each condition (pH 3, and 13), one of the species between protonated and deprotonated is remarkably dominant. Therefore, we considered that the spectrum at pH 3 is a result of full protonation, and the spectrum at 13 is a result of full deprotonation. Based on the assumption, we calculated the ratio between the forms from the spectra in each condition.

$$I(\lambda) = A_1 e^{-\frac{(\lambda - x_{c1})^2}{2{\sigma_1}^2}} + A_2 e^{-\frac{(\lambda - x_{c2})^2}{2{\sigma_2}^2}}, \quad (13)$$

$$(A: Area, x_c: center\ of\ gaussian, \sigma: width, \lambda: wavelength)$$

In the second step, we calculated the ratio between protonated and deprotonated forms using the two model spectra obtained in the first step. Fitting two model curves using equation 14 derived the ratios of the components in different pH conditions. All the R^2 values were over 0.90 (Table S1).

$$I_{total}(\lambda) = W_1 I_1(\lambda) + W_2 I_2(\lambda) \quad (14)$$

$$(W: Weighting\ factor)$$

pH	R^2
3	0.91
5	0.94
6	0.95
7.4	0.95
9	0.92
11	0.90
13	0.92

Table S1. The values of R^2 in different pH conditions. The values confirmed the precision of fittings.

4.2. pH-dependent size changes

4.2.1. pH-dependent size changes observed by dynamic light scattering (DLS)

Sizes of the molecular biodynamer in different pH conditions were measured using DLS. The biodynamer stock solution (10 mM, in 10 mM acetate buffer, pH 5.0) was diluted to 1 mg/mL using 10 mM phosphate solution (pH 7.4 and 13) or 10 mM acetate solution (pH 3.0 and 5.0). After the dilution, the addition of 10 M NaOH and 1 M HCl adjusted their pH exactly to 3, 5, 7.4, and 13. Each of the particles was measured using Zetasizer Nano ZSP (Malvern Instruments, Malvern, United Kingdom), observed from 173° backlight scattering.

4.2.2. pH-dependent size changes observed by static light scattering (SLS)

1 mg/mL of biodynamer solution at pH 5.0 (10 mM acetate buffer) and pH 7.4 (10 mM phosphate buffer) was measured using SLS. The measurement and analysis details are described in 3.4.

References

1. J. F. Folmer-Andersen, E. Buhler, S.-J. Candau, S. Joulie, M. Schmutz, J.-M. Lehn, Cooperative, bottom-up generation of rigid-rod nanostructures through dynamic polymer chemistry, *Polym. Int.* **2010**, *59*, 1477-1491.
2. D. A. Patrick, D. W. Boykin, W. D. Wilson, F. A. Tanious, J. Spychala, B. C. Bender, J. E. Hall, C. C. Dykstra, K. A. Ohemeng, R. R. Tidwell, Anti-Pneumocystis carinii pneumonia activity of dicationic carbazoles, *Eur. J. Med. Chem.* **1997,** *32*, 781-793.
3. Y. Liu, M. C. A. Stuart, E. Buhler, J.-M. Lehn, A. K. H. Hirsch, Proteoid Dynamers with Tunable Properties, *Adv. Funct. Mater.* **2016**, *26*, 6297-6305.
4. G. Marinani, E. Buhler, I. J. R. Colard, D. Dattler, N. Giuseppone, E. Moulin, S. Prevost, Effects of polymer molecular weight on the structure and on the efficiency of light-driven contractile gels, Institut Laue-Langevin (ILL), **2019**, doi: doi.ill.fr/10.5291/ILL-DATA.9-11-1845.
5. G. Mariani, A. Goujon, E. Moulin, M. Rawiso, N. Giuseppone, E. Buhler, Integration of molecular machines into supramolecular materials: actuation between equilibrium polymers and crystal-like gels, *Nanoscale,* **2017**, *9*, 18456-18466.
6. H. Zhao, P. H. Brown and P. Schuck, On the distribution of protein refractive index increments, *Biophys. J.*, **2011**, *100*, 2309-2317.
7. Y. Liu, M. C. A. Stuart, M. D. Witte, E. Buhler, A. K. H. Hirsch, Saccharide-Containing Dynamic Proteoids, *Chem. Eur. J.* **2017**, *23*, 16162-16166.
8. Y. Liu, M. C. A. Stuart, E. Buhler, A. K. H. Hirsch, Dynamic Proteoids Generated From Dipeptide-Based Monomers, *Macromol. Rapid Commun.* **2018**, *39*, 1800099.